AGU PUBLICATIONS

Geophysical Research Letters

RESEARCH LETTER
10.1002/2013GL059149

Key Points:
- Near-surface shear must be considered in parameterizations of eddy viscosity
- Wind stress-dependent eddy viscosities may result in biased estimates of shear
- Eddy viscosity models that explicitly include the mean shear are proposed

Supporting Information:
- Readme
- Figure S1
- Figure S2

Correspondence to:
J. O. Wenegrat,
wenegrat@uw.edu

Citation:
Wenegrat, J. O., M. J. McPhaden, and R.-C. Lien (2014), Wind stress and near-surface shear in the equatorial Atlantic Ocean, *Geophys. Res. Lett.*, *41*, 1226–1231, doi:10.1002/2013GL059149.

Received 25 DEC 2013
Accepted 10 JAN 2014
Accepted article online 31 JAN 2014
Published online 19 FEB 2014

Wind stress and near-surface shear in the equatorial Atlantic Ocean

Jacob O. Wenegrat[1], Michael J. McPhaden[1,2], and Ren-Chieh Lien[1,3]

[1]School of Oceanography, University of Washington, Seattle, Washington, USA, [2]Pacific Marine Environmental Laboratory, NOAA, Seattle, Washington, USA, [3]Applied Physics Laboratory, University of Washington, Seattle, Washington, USA

Abstract The upper ocean response to wind stress is examined using 8 months of unique near-surface moored velocity, temperature, and salinity data at 0°N, 23°W in the equatorial Atlantic. The effects of wind stress and shear on the time-varying eddy viscosity are inferred using the surface shear-stress boundary condition. Parameterizations of eddy viscosity as a function of wind stress and shear versus wind stress alone are then examined. In principle, eddy viscosity should be proportional to the inverse shear, but how it is represented implicitly or explicitly can affect estimates of the near-surface flow field. This result may explain some discrepancies that have arisen from using parameterizations based only on wind stress to characterize the effects of turbulent momentum mixing.

1. Introduction

The turbulent vertical flux of wind-driven momentum plays a crucial role in the near-surface momentum budget [*Smyth et al*., 1996] and is critical for accurate understanding and modeling of near-surface currents. This is particularly important at low latitudes, where diminished rotational constraints increase the sensitivity of modeled currents and sea surface temperature to vertical mixing [*Schneider and Müller*, 1994]. Most commonly, the Reynolds stress is approximated by assuming down-gradient transport by turbulence, parameterized by a turbulent eddy viscosity, denoted A_v. Closing the equations of motion then becomes a task of correctly parameterizing A_v as a function of known variables.

Ultimately, accurate parameterizations of near-surface A_v need to account for a wide-variety of physical processes, including shear instabilities, thermal convection, Langmuir circulation, and wave breaking [cf. *Sullivan and McWilliams*, 2010]. However, a simple approach that is often applied within the unstratified surface mixed layer, where Richardson number-dependent parameterizations are not applicable, is to parameterize A_v as a function of the wind stress alone. This approach has a long history in the literature, dating back to *Ekman* [1905] and, more recently, *Santiago-Mandujano and Firing* [1990, *hereinafter SF90*]. The simplicity of this type of parameterization lends itself well to analytic studies of the Ekman layer [*Cronin and Kessler*, 2009] or in applications where detailed upper ocean data are lacking, such as with the Ocean Surface Current Analysis-Real Time (OSCAR) surface current product [*Bonjean and Lagerloef*, 2002], which utilizes only remotely sensed data.

Despite the widespread use of wind stress parameterizations of A_v, the literature contains a large spread of coefficients [*Huang*, 1979; *SF90*] and lacks clarity on their appropriate usage. Progress on this topic has been hampered by the relative scarcity of observations of near-surface velocity, as shipboard current profilers are limited by ship draft and moored upward facing acoustic Doppler current profilers (ADCPs) are subject to surface reflection effects. Here we utilize a unique data set from a moored downward facing ADCP in the equatorial Atlantic, providing both high vertical resolution and an extended time series of near-surface velocity. Using these data, we infer an eddy viscosity based on wind stress data and near-surface shear and examine three parameterizations. Model 1 is based on regression analysis using only wind stress, following *SF90*. Models 2 and 3 are formulated explicitly to include the mean shear, which improves their generality and may lead to significantly more accurate modeling of near-surface flow.

2. Data and Methods

As part of an engineering comparison of current meters, a 600 kHz ADCP was deployed at the 0°N, 23°W Prediction and Research Moored Array in the Tropical Atlantic [*Bourlès et al*., 2008] mooring from 13 October

2008 through 18 June 2009. The ADCP was deployed facing downward on the mooring bridle and returned data in 0.75 m vertical bins between $z = -3.76$ m and $z = -38.26$ m (supporting information Figures S1b and S1c). To limit the effect of mooring motion due to surface waves, each velocity datum was recorded as the ensemble average of 120 consecutive 1 Hz samples, once per hour at the top of the hour.

Several ADCP velocity bins were biased by sidelobe reflection off instruments on the mooring line. Corrupted bins were identified visually based on discontinuities in profiles of echo intensity and velocity and were removed from the data. Data collected during 14–15 October 2008 and 18–19 March 2009 were particularly noisy and consequently excluded from the analysis. ADCP velocity data were compared with point current meters located at depths of 6, 10, 17, 20, and 26 m. After correction for a systematic bias in the ADCP compass headings, the hourly zonal (meridional) interpolated ADCP velocities compared favorably with the point current meters, with correlation coefficient $r = 0.994$ ($r = 0.985$) and RMS differences of 0.032 m s^{-1} (0.038 m s^{-1}) at 6 m depth.

Near-surface shear was calculated by forward differencing between $z = -3.76$ m and $z = -7.51$ m, the uppermost uncorrupted bins, giving a nominal depth for the uppermost shear bin of 5.64 m (Figure S1d). A white-noise threshold for shear was determined from the spectra of shear components by taking the average spectral level (S) from 4.8 cycles per day (cpd) to the Nyquist frequency (NF) and estimating the RMS shear error as $\sigma_E = [S \times \mathrm{NF}]^{\frac{1}{2}}$. For the hourly shear magnitude, $\sigma_E = 1.2 \times 10^{-2} \mathrm{s}^{-1}$, consistent with estimates derived from RMS differences between the point current meters and the ADCP.

Temperature and salinity were recorded every 10 min, at depths of 1, 5, 10, 13, 20, 23, 40, and 60 m and 1, 5, 20, 40, and 60 m, respectively. The 1 m salinity data were only returned for the first 22 days of the record. During this period the hourly 5 m salinity values were highly correlated with the 1 m values ($R^2 = 0.98$); hence, linear regression was used to fill the missing 1 m salinity data using the 5 m observations for the remainder of the record. Density was then calculated using hourly averaged data and linearly interpolated to a uniform grid (Figure S1e). Mixed layer depth was defined as the depth at which the density first exceeds the 1 m density by 0.125 kg m^{-3} [*Levitus*, 1982].

Wind stress was calculated from mooring observations of wind speed at 4 m height (Figure S1a), using the COARE 3.0b algorithm [*Fairall et al*., 2003]. We consider A_v parameterizations formulated as functions of the wind stress, rather than the wind speed. This approach is most general and avoids issues of consistency in the choice of wind stress parameterizations when the A_v parameterization is applied to new data sets. Where necessary for comparison with prior work, we approximate the conversion between wind speed and wind stress as $\vec{\tau} = \rho_{\mathrm{air}} C_d \left|\vec{U}\right| \vec{U}$, where $\vec{U}$ is the wind velocity vector at 10 m, $\rho_{\mathrm{air}} = 1.18$ kg m^{-3}, and $C_d = 1.14 \times 10^{-3}$ chosen for consistency with *SF90*.

Observations where the velocity shear and wind stress components are of opposite signs (implying a negative A_v), where A_v exceeds 0.045 m^2 s^{-1}, the 99th percentile estimated using the bootstrap method, or where the uppermost bin of shear is below the mixed layer, were excluded from analysis.

3. Results

3.1. Eddy Viscosity

Continuity across the air-sea interface requires that the surface ocean stress match the wind stress. This leads to the standard surface boundary condition, $\rho A_v \vec{u}_z = \vec{\tau}$ for $z = 0$, where ρ is the density of seawater, $\vec{u}$ the horizontal velocity vector, z the vertical coordinate defined positive upward, $\vec{\tau}$ the wind stress vector, and subscript z denotes differentiation. Assuming wind stress and shear are aligned (discussed below), the boundary condition can be rearranged to give a formula for A_v,

$$A_v = \frac{\tau}{\rho u_z} \quad \text{for} \quad z = 0 \tag{1}$$

where the vector notation has been dropped to indicate vector magnitudes.

We evaluate (1) using hourly wind stress and shear, assuming uniform stress in a layer between the surface and 5.64 m. Observational evidence suggests that near-surface stress profiles decay smoothly from the surface wind stress value [*Smyth et al*., 1996]; however, temporal variability of the vertical structure of near-surface stress is not well understood and may be a function of Richardson number [*Soloviev et al*., 2001] or free-surface effects [*McWilliams et al*., 2012]. Assuming a linear decay of stress between the surface and the

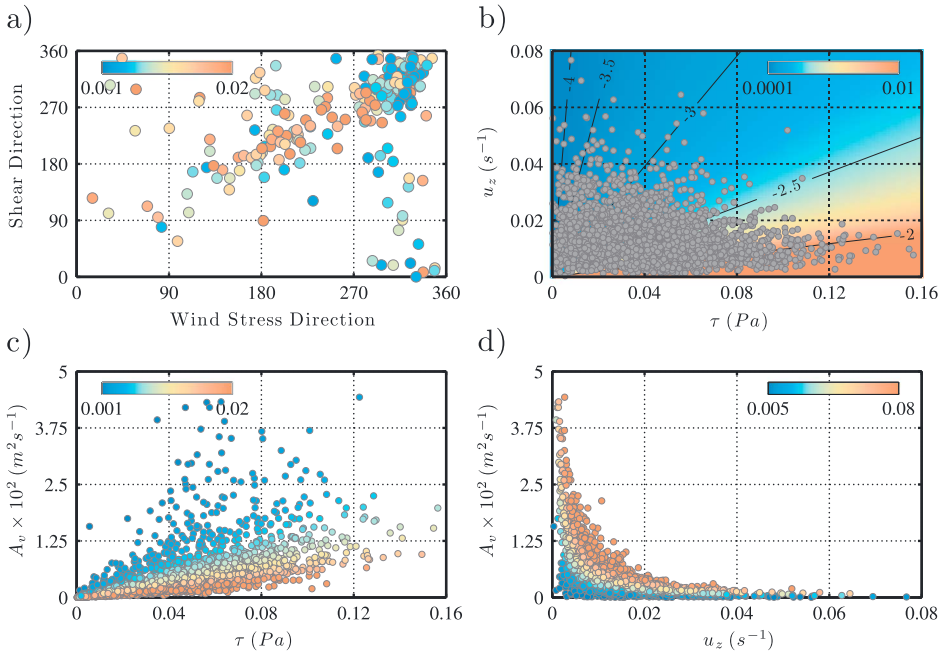

Figure 1. (a) Daily averaged shear direction versus wind stress direction with shear magnitude (color scale, s^{-1}); (b) hourly shear magnitude versus wind stress magnitude, superimposed over the value of A_v predicted by 1 (color scale, $m^2 s^{-1}$, and log contours); (c) A_v versus wind stress, with shear magnitude (color scale, s^{-1}), (d) A_v versus shear, with wind stress magnitude (color scale, Pa).

thermocline [*Hebert et al.*, 1991; *Smyth et al.*, 1996], the average stress at 5.64 m will be 92% of the surface stress, which does not materially alter our analysis. Given this, we do not attempt to correct for a decaying near-surface stress profile and proceed with the assumption of a uniform stress layer. Free-surface effects may modify the shear profile near the surface; thus, the value of A_v we infer is most conservatively treated as the 5.64 m value.

Daily values of the shear direction are generally aligned with the wind stress direction (Figure 1a), although greater scatter is observed in hourly values. Misalignment between wind stress and shear would suggest a vector A_v. However, as (1) still defines the magnitude of A_v, we do not further consider the directionality of A_v here. Consistent with *SF90*, we find that the shear magnitude is not well correlated with the wind stress magnitude (Figure 1b), confirming that A_v must be a time-varying quantity in order to fulfill the surface boundary condition. Observations span several decades of magnitude of A_v (Figure 1b, color scale), with comparable variance in each dimension.

The variance of A_v can be approximated using the first-order Taylor expansion of (1), giving $Var(A_v) \approx \frac{\overline{\tau}^2}{\rho^2 \overline{u_z}^2}\left(\frac{Var(\tau)}{\overline{\tau}^2} - \frac{2Cov(\tau,u_z)}{\overline{\tau}\,\overline{u}_z} + \frac{Var(u_z)}{\overline{u_z}^2}\right)$, where overbars denote mean values. The first and third terms on the right-hand side are comparable in magnitude, and together are approximately 5 times larger than the covariance term. Two-dimensional projections of A_v as a function of each independent variable (Figures 1c and 1d) also emphasize that although A_v can be approximated as a univariate function of either stress or shear, both independent variables contribute to the true A_v. The accuracy of wind stress-only parameterizations will decline with increasing shear variance, and so, before discussing parameterizations, we characterize the variability of the shear.

3.2. Shear Variability

Figure 2 shows the variance-preserving spectra of the wind stress and shear components. Each component is normalized by the square of its time domain mean, as it appears in the first-order Taylor series expansion of the A_v variance (section 3.1), allowing a frequency domain estimate of the relative contribution of each variable to the eddy viscosity. At the lowest frequencies, variability is dominated by the wind stress, with comparable contributions from both shear and stress between frequencies of approximately 0.05 to 0.8 cpd, above which shear variance surpasses stress variance. Wind stress-only parameterizations are thus expected

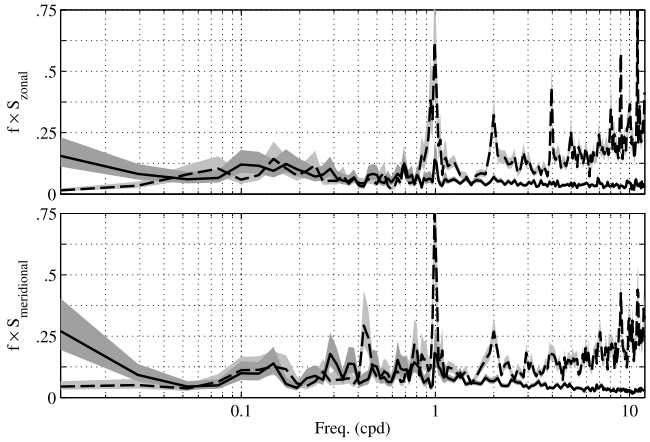

Figure 2. Variance-preserving spectra for (top) zonal and (bottom) meridional components of wind stress (solid line) and shear at 5.64 m (dashed line), with 95% confidence intervals (shaded area). Both shear and stress spectra are nondimensionalized as discussed in section 3.2.

to perform best at the lowest frequencies, where the relative shear variance is low, and to miss significant portions of the true variance at frequencies at or above 0.05 cpd, where the shear variance increases.

Shallow mixed layers were found to be associated with both increased variability and mean values of near-surface shear (Figure 3). This is believed to result from both the formation of an afternoon near-surface stratified diurnal jet [*Price et al.*, 1986] and the vertical advection of the high-shear region on the upper flank of the equatorial undercurrent during periods of low wind stress (Figure 3, color scale, and Figure S1). Consequently, for the equatorial region, wind stress-only parameterizations may not be appropriate in the case of shallow mixed layers or low wind stress. Alternatively, our assumption of uniform stress between the surface and 5.64 m may be violated when the mixed layer is shallow. Attempts to relate shear to other physical variables such as the thermocline depth or the Monin-Obukhov length were unsuccessful.

Next, we consider three models that parameterize A_v as a function of wind stress.

3.3. Model 1: Wind Stress Only

Previously, parameterizations of A_v as a function of wind stress alone have specified a model of the form $A_v = \beta\tau$, where β is estimated by least squares regression. When an intercept term is included, it is found to not be significantly different than zero, as anticipated from (1), and we proceed using regression through the origin, which produces the following estimate of the coefficient:

$$\hat{\beta} = \frac{\Sigma \tau A_v}{\Sigma \tau^2} = \frac{1}{\rho}\overline{\left(\frac{1}{u_z}\right)} + \frac{\mathrm{Cov}(\tau^2, u_z^{-1})}{\rho \overline{\tau^2}} \tag{2}$$

For our data set, $\hat{\beta} = 0.113\ \ \mathrm{m^2 s^{-1} Pa^{-1}}$ (Table 1 and Figure S2), similar to that of *SF90*. We note that *SF90* also considered a regression based on the logarithm of (1); however, in the wind ranges considered here (0–10 m $\mathrm{s^{-1}}$), the two formulations are very similar.

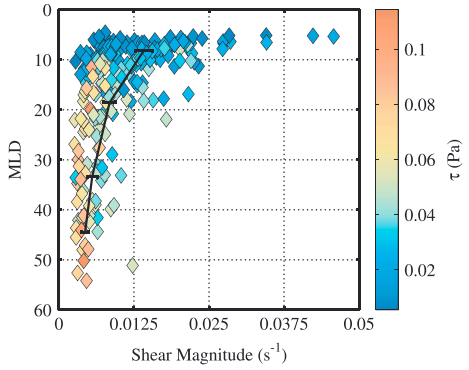

Figure 3. Daily shear magnitude at 5.64 m versus mixed layer depth (scatter), binned mean shear with 95% confidence intervals based on a one-sample t-test (solid line), and daily wind stress magnitude (color scale).

3.4. Model 2: Mean Inverse Shear

In our data set, the correlation between inverse shear and squared stress is weak; thus, a simple and transparent estimate for β is given by

$$\overline{\beta} = \frac{1}{\rho}\overline{\frac{1}{u_z}} \tag{3}$$

In the case of completely uncorrelated inverse shear and squared stress (3) is exactly equivalent to (2), and our estimate $\overline{\beta} = 0.108\ \ \mathrm{m^2 s^{-1} Pa^{-1}}$ is within the confidence intervals of our estimate of $\hat{\beta}$ (Table 1 and Figure S2). Model 2 has the advantage of explicitly including the dependence on the mean inverse shear, a dependence that is obscured in regression-based coefficients.

Table 1. Summary of Model Parameters[a]

	$\beta \times 10^2$	R^2_a	R^2_b	SE $\times 10^3$	NRMSE
Model 1	11.3 (10.8, 11.9)	0.61	0.33	2.54	1.18
Model 2	10.8 (10.3, 11.4)	0.56	0.33	2.54	1.16
Model 3	6.59 (5.50, 7.67)	0.21	0.14	2.99	1.00
*SF*90	8.9	0.38	0.28	2.65	1.07

[a] β ($m^2\,s^{-1}\,Pa^{-1}$) coefficients with 95% confidence intervals is calculated using the wild bootstrap method; $R^2{}_a$ is the coefficient of determination for regression through the origin [*Eisenhauer*, 2003]; $R^2{}_b$ is the standard squared correlation coefficient; SE is the heteroscedastic-consistent standard error ($m^2\,s^{-1}$) [*Cribari-Neto*, 2004]; and NRMSE is the RMS error of the estimated shear, normalized by the standard deviation.

3.5. Model 3: Mean Shear

One important consequence of utilizing a parameterization where A_v is directly proportional to the wind stress is that it follows immediately from (1) that $u_z = (\rho\beta)^{-1}$. Hence, the estimated surface shear magnitude is assumed constant by definition. Generally, $\overline{u}_z \neq \left(\overline{u_z^{-1}}\right)^{-1}$, so the shear calculated using model 1, or 2, will be biased relative to the true shear. This argues for the parameterization

$$\widetilde{\beta} = \frac{1}{\rho}\frac{1}{\overline{u}_z} \tag{4}$$

which is the first term in a Taylor expansion of (1), exact only when the true shear is constant. Table 1 shows that by traditional measures model 3 underperforms the other models, and additionally, we note that it is the most biased of the models for A_v (Figure S2). However, model 3 minimizes $\sum (u_z - (\rho\beta)^{-1})^2$, the mean square error of shear estimated using the surface boundary condition, desirable for modeling surface currents. This is discussed further below.

4. Discussion

In the absence of detailed upper ocean data it is often necessary to rely on very simple parameterizations of A_v, and wind stress-only parameterizations have a history in the literature of over a century and remain an appealing goal [*Huang*, 1979]. However, wind stress-only parameterizations, of any form, imply $u_z = \tau[\rho A_v(\tau)]^{-1}$, or equivalently $u_z = f(\tau)$. Without the inclusion of additional parameters to constrain the relationship between shear and stress, Figure 1b suggests that the best possible choice may simply be constant u_z, which implies $A_v \propto \tau$. Within the framework of Ekman dynamics, this can be understood as the boundary layer depth adjusting to the wind stress, maintaining constant near-surface shear. Our analysis suggests that this form of parameterization may not be accurate at frequencies above 0.05 cpd, and in the case of shallow mixed layers and low wind stress.

Examining the algebraic statement for the regression coefficient, (2) highlights the first-order dependence on the mean inverse shear. Thus, discrepancies in published coefficients for wind stress-only parameterizations could result simply from the different mean shears across observations, a fact that also raises doubts about the generality of these parameterizations. Accordingly, rather than relying on published coefficients, it is preferable to use some local estimate of the mean shear which might come from either in situ or historical data when available. A high correlation between monthly averaged bulk shear and bulk stratification over the upper 30 m ($R^2 = 0.80$) is consistent with the observed relationship between shear and mixed layer depth (section 3.2) and suggests the possibility that in situ stratification data might be used to infer an expected near-surface shear when no direct estimate is available, a form of Richardson number closure [cf. *Pollard et al.*, 1972; *Price et al.*, 1986; *Ralph and Niiler*, 1999].

Coefficients proportional to the mean inverse shear, as is implicit in regression-based models, result in considerably biased estimates of the surface shear. Comparing the OSCAR model, which is based on the analytical model of *Bonjean and Lagerloef* [2002] and utilizes the *SF90* parameterization for equatorial A_v, to our data set reveals a 25 cm s^{-1} eastward bias in the OSCAR currents. This is consistent with a recently identified eastward bias in the OSCAR climatology throughout the equatorial Atlantic and Pacific Oceans [*Lumpkin and Johnson*, 2013]. For this data set model 3 implies surface shears 35% larger than *SF90*, suggesting that a portion of the observed bias may be related to the choice of A_v parameterization. However, velocity errors are sensitive to both the surface value and the vertical profile of shear, highlighting the need for further study of the vertical structure of A_v in the near surface layer.

Acknowledgments
The authors thank Patricia Plimpton for the initial processing of ADCP data, and two anonymous reviewers for their critical reading and feedback. J. O. W. and M. J. M. were supported by NOAA, and R.-C. L. was supported by NSF grant OCE1029488. PMEL contribution 4020 and JISAO contribution 2120.

The Editor thanks two anonymous reviewers for their assistance in evaluating this paper.

References

Bonjean, F., and G. S. E. Lagerloef (2002), Diagnostic model and analysis of the surface currents in the tropical Pacific Ocean, *J. Phys. Oceanogr.*, *32*(10), 2938–2954, doi:10.1175/1520-0485(2002)032<2938:DMAAOT>2.0.CO;2.

Bourlès, B., et al. (2008), The PIRATA Program: History, accomplishments, and future directions, *Bull. Am. Meteorol. Soc.*, *89*(8), 1111–1125, doi:10.1175/2008BAMS2462.1.

Cribari-Neto, F. (2004), Asymptotic inference under heteroskedasticity of unknown form, *Comput. Stat. Data Anal.*, *45*(2), 215–233, doi:10.1016/S0167-9473(02)00366-3.

Cronin, M. F., and W. S. Kessler (2009), Near-surface shear flow in the tropical Pacific cold tongue front, *J. Phys. Oceanogr.*, *39*(5), 1200–1215, doi:10.1175/2008JPO4064.1.

Eisenhauer, J. G. (2003), Regression through the origin, *Teach. Stat.*, *25*(3), 76–80, doi:10.1111/1467-9639.00136.

Ekman, V. W. (1905), *On the Influence of the Earth's Rotation on Ocean-Currents*, Ark. Mat. Astron. Fys., Uppsala, Sweden.

Fairall, C. W., E. F. Bradley, J. E. Hare, A. A. Grachev, and J. B. Edson (2003), Bulk parameterization of air–sea fluxes: Updates and verification for the COARE algorithm, *J. Clim.*, *16*(4), 571–591, doi:10.1175/1520-0442(2003)016<0571:BPOASF>2.0.CO;2.

Hebert, D., J. N. Moum, C. A. Paulson, D. R. Caldwell, T. K. Chereskin, and M. J. McPhaden (1991), The role of the turbulent stress divergence in the equatorial Pacific zonal momentum balance, *J. Geophys. Res.*, *96*(C4), 7127–7136, doi:10.1029/91JC00271.

Huang, N. E. (1979), On surface drift currents in the ocean, *J. Fluid Mech.*, *91*(01), 191–208, doi:10.1017/S0022112079000112.

Levitus, S. (1982), *Climatological Atlas of the World Ocean*, NOAA Prof. Paper No. 13, U.S. Govt. Printing Office, Washington, D. C.

Lumpkin, R., and G. C. Johnson (2013), Global ocean surface velocities from drifters: Mean, variance, El Niño-Southern Oscillation response, and seasonal cycle, *J. Geophys. Res. Oceans*, *118*, 2992–3006, doi:10.1002/jgrc.20210.

McWilliams, J. C., E. Huckle, J.-H. Liang, and P. P. Sullivan (2012), The wavy Ekman layer: Langmuir circulations, breaking waves, and Reynolds stress, *J. Phys. Oceanogr.*, *42*(11), 1793–1816, doi:10.1175/JPO-D-12-07.1.

Pollard, R. T., P. B. Rhines, and R. O. R. Y. Thompson (1972), The deepening of the wind-mixed layer, *Geophys. Fluid Dyn.*, *4*(1), 381–404.

Price, J. F., R. A. Weller, and R. Pinkel (1986), Diurnal cycling: Observations and models of the upper ocean response to diurnal heating, cooling, and wind mixing, *J. Geophys. Res.*, *91*(C7), 8411–8427, doi:10.1029/JC091iC07p08411.

Ralph, E. A., and P. P. Niiler (1999), Wind-driven currents in the tropical Pacific, *J. Phys. Oceanogr.*, *29*(9), 2121–2129, doi:10.1175/1520-0485(1999)029<2121:WDCITT>2.0.CO;2.

Santiago-Mandujano, F., and E. Firing (1990), Mixed-layer shear generated by wind stress in the central equatorial Pacific, *J. Phys. Oceanogr.*, *20*(10), 1576–1582, doi:10.1175/1520-0485(1990)020<1576:MLSGBW>2.0.CO;2.

Schneider, N., and P. Müller (1994), Sensitivity of the surface equatorial Ocean to the parameterization of vertical mixing, *J. Phys. Oceanogr.*, *24*(7), 1623–1640, doi:10.1175/1520-0485(1994)024<1623:SOTSEO>2.0.CO;2.

Smyth, W. D., D. Hebert, and J. N. Moum (1996), Local ocean response to a multiphase westerly wind burst: 1. Dynamic response, *J. Geophys. Res.*, *101*(C10), 22495–22512, doi:10.1029/96JC02005.

Soloviev, A., R. Lukas, and P. Hacker (2001), An approach to parameterization of the oceanic turbulent boundary layer in the western Pacific warm pool, *J. Geophys. Res.*, *106*(C3), 4421–4435, doi:10.1029/2000JC900154.

Sullivan, P. P., and J. C. McWilliams (2010), Dynamics of winds and currents coupled to surface waves, *Annu. Rev. Fluid Mech.*, *42*(1), 19–42, doi:10.1146/annurev-fluid-121108-145541.